On the Physical Interpretation of the Saleh–Valenzuela Model and the Definition of Its Power Delay Profiles

Arjan Meijerink, *Senior Member, IEEE*, and Andreas F. Molisch, *Fellow, IEEE*

***Abstract*—The physical motivation and interpretation of the stochastic propagation channel model of Saleh and Valenzuela are discussed in detail. This motivation mainly relies on assumptions on the stochastic properties of the positions of transmitter, receiver and scatterers in the propagation environment, and on the frequency range that is covered by the model. Some of these assumptions break down when the application of the model is extended from wideband to ultra-wideband propagation channels. Another important difference between these application contexts is the spatial scale over which the stochastic properties of the channel fluctuate when the transmitter or receiver is moved. This is further illustrated by analyzing the average power delay profile and some other channel properties for different levels of ensemble averaging, and discussing the relation between the ensemble averaging levels and the spatial variation scales. The notion of the averaging levels is essential for correct interpretation of the model, and hence for appropriate channel characterization and system design.**

***Index Terms*—Delay dispersion, Saleh–Valenzuela (SV) model, stochastic channel model, ultra-wideband (UWB), wireless propagation.**

I. Introduction

THE Saleh–Valenzuela (SV) model [1] is a popular and widely accepted propagation model that describes the stochastic properties of the arrival delays and amplitudes of resolvable multipath components (MPCs) in indoor wideband (WB) wireless transmission systems. It models the arrivals of MPCs in clusters, where both the cluster arrivals and the arrivals of MPCs within each cluster are assumed to be governed by Poisson processes.

The SV model was originally introduced within the context of WB systems with bandwidths in the order of a few hundred MHz. Later it was found that measurements of ultra-wideband (UWB) channels also fit the SV model well. It was used as the basis for the IEEE 802.15.3a model [2], [3], which was developed in order to compare standardization proposals for high-data-rate wireless personal area networks (PANs). Later, a modified SV model was introduced and used in the IEEE 802.15.4a model [4], [5], for low-data-rate wireless PANs with ranging capability. Extensive measurement campaigns were performed to parametrize the models for different scenarios, such as residential, office, industrial, and outdoor environments. For all scenarios (except outdoor), the models were separately parametrized for line-of-sight (LOS) and non-line-of-sight (NLOS) conditions. The measurements were performed in various frequency ranges, all in the order of a few GHz wide, and various distance ranges, all in the order of several meters up to a few tens of meters.

Nevertheless, the actual extension from WB to UWB in the development of the IEEE 802.15.3a and 802.15.4a channel models was performed in a rather ad-hoc fashion. That is, instead of reconsidering the physical assumptions that led to the WB SV model, verifying whether these also hold in the UWB case, and possibly adapting according to physical reasoning, the actual model extensions were mostly based on empirical data from channel measurements. Although at that time this seemed the best way to quickly obtain acceptable tools for benchmarking candidate technologies for the standards, this approach limits the actual understanding of the physical effects in WB and UWB channels. Therefore care must be taken when using the same models for other purposes.

One of the essential differences between WB systems and UWB systems is the spatial scale over which the statistical properties of the channel change when the position of the transmitter (Tx) and/or receiver (Rx) is varied. For instance, the derivation of fading statistics in WB channels is based on the assumption that the position of the Tx or Rx can be varied on such a scale that the MPC amplitudes change while the other random parameters (most notably the MPC arrival delays) remain constant. However, this assumption no longer holds for UWB channels with a large relative bandwidth [6]. Therefore, it is of utmost importance to clearly specify the spatial scale over which measurements are taken, and when these results are combined and related to analytical statistics (for instance expected values), it should be explicitly specified which parameters are varied (or "averaged out"), and which parameters are kept constant. Especially this latter aspect is sometimes described somewhat obscurely in literature on SV-based channel models. The analytical statistics are in fact conditional statistics (which are only locally valid), but it is often unclear on which random parameters these statistics are conditioned. Nevertheless, proper understanding of these conditional statistics and the local estimation of the corresponding parameters (such as described in [7]) is essential for proper design of for instance adaptive equalization and/or diversity schemes.

Manuscript received November 15, 2013; revised June 22, 2014; accepted June 22, 2014. Date of publication July 08, 2014; date of current version September 01, 2014. Part of the work of A. Meijerink was performed while visiting the University of Southern California and supported by Agentschap NL through the Point One project ALwEN (PNE07007). The work of A. F. Molisch was supported in part by the National Science Foundation and by the Office of Naval Research.

A. Meijerink is with the Telecommunication Engineering Group, Faculty of Electrical Engineering, Mathematics and Computer Science, University of Twente, 7500 AE, Enschede, The Netherlands (e-mail: a.meijerink@ieee.org).

A. F. Molisch is with the Ming Hsieh Department of Electrical Engineering, University of Southern California, Los Angeles, CA 90089 USA (e-mail: andreas.molisch@ieee.org).

Digital Object Identifier 10.1109/TAP.2014.2335812

Moreover, the actual link between statistical and spatial fluctuations is something that can be questioned. In other words, can the fluctuations of the random parameters as a function of the position (of the Tx or Rx) be considered as a *spatially ergodic process*? This is an essential question when model parameters are derived from measurements.

The aim of this paper is two-fold. First of all, it aims to conduct a thorough discussion on the physical assumptions that were made upon definition of the SV model (mainly focusing on geometrical considerations), and why these assumptions partly break down when the model is applied in a UWB context instead of a WB context. Second, explicit definitions of the conditional statistics of several properties of the SV model will be given and discussed. Specifically, it will be explained what different levels of expectation and spatial averaging can be distinguished when calculating or measuring these properties, respectively, and how the ordering of these levels is influenced by the extension from WB to UWB. Analytical expressions for the average power delay profile (PDP) and several other channel properties will be presented for different levels of ensemble averaging, and it will be discussed how these results should be interpreted and linked to the physical motivation for the model. Furthermore it will be discussed if and how these results can be related to practical measurements, and what this implies for the way in which the model parameters are extracted from measurements, and for the way in which the model is applied in system design and performance evaluation, especially when UWB channels are considered.

The paper is outlined as follows. The origin, structure and physical motivation of the SV model are described in Section II. Then, in Section III, it is discussed how the physical motivation of the model breaks down when extending its application from WB to UWB, and how this extension influences the ordering of the spatial variation levels. In Section IV this is further illustrated by analyzing the model in terms of the PDP and several other channel properties, for different ensemble averaging levels, and linking these levels to the spatial variation levels. Conclusion are formulated in Section V.

II. Origin, Structure and Physical Motivation of the Saleh–Valenzuela Model

A. Turin's Poisson Arrival Model

The SV model was mainly inspired by the pioneering work of Turin, who postulated that the received signal in a static WB wireless communication system can be written as the sum of undistorted replicas (the MPCs) of the transmitted signal [8] (i.e., only delayed, attenuated and shifted in phase). In other words, in each point of a three-dimensional environment, the propagation channel can be characterized by a linear time-invariant filter with a complex baseband equivalent impulse response that can be written as

$$h(\tau) = \sum_{k=0}^{\infty} \beta_k \, \exp(\mathrm{j}\,\phi_k)\, \delta(\tau - \tau_k) \tag{1}$$

where β_k, ϕ_k, and τ_k are the random amplitude, phase and propagation delay of the kth MPC, and $\delta(\,\cdot\,)$ is the Dirac delta function.[1]

Turin *et al.* conjectured that, in urban environments, the propagation delays $\{\tau_k\}$ can be described as a homogeneous Poisson sequence [9]. Mathematically, this can be described in three ways.

1) The number of MPC arrivals N in any delay interval of length T after the arrival of the first MPC is Poisson-distributed with mean λT, i.e.,

$$\mathrm{P}[N = n] = \frac{(\lambda T)^n \exp(-\lambda T)}{n!}, \quad n = 0, 1, 2, \ldots, \tag{2}$$

where λ is the mean arrival rate, and the numbers of MPC arrivals in disjoint delay intervals are mutually independent.

2) The number of MPC arrivals N in any delay interval of length T after the arrival of the first MPC is Poisson-distributed with mean λT, and, given N, the unordered MPCs have mutually independent arrival delays, each uniformly distributed in that interval.

3) When the MPCs are ordered according to the values of their arrival delays, the differences between the arrival delays of successive MPCs are exponentially distributed and mutually independent, i.e., the arrival delays can be written as

$$\tau_k = \tau_0 + \sum_{m=1}^{k} \Delta\tau_m \tag{3}$$

where τ_0 is the (known) arrival delay of the first component (we will come back to this later) and the interarrival delays have probability density

$$p_{\Delta\tau_k}(\tau) = \lambda \, \exp(-\lambda\tau), \quad \tau > 0\,. \tag{4}$$

The rationale for this conjecture was that the scatterers, i.e., the objects introducing the MPCs, can be assumed to be completely randomly located in space. To be precise, if one assumes that each scatterer introduces one resolvable MPC (and that each MPC reflects upon only one scatterer), and that the positions of the reflection points form a spatial Poisson process, then, for given Tx and Rx positions, it follows from geometrical considerations[2] that the MPC arrivals follow a Poisson process. When

[1]Strictly speaking, the (continuous-time) impulse response of *any* linear time-invariant system can be approximated by a summation of delta functions, where the approximation can be made arbitrarily accurate by spacing the delta functions sufficiently closely, given the bandwidth of the input signal. The main added value of such a notation in a wireless propagation model is its appealing interpretation, where each delta function corresponds to one MPC (or a set of nonresolvable MPCs). This is particularly useful in time-*variant* systems, where tiny variations in the positions of the Tx, Rx and/or scatterers may lead to a change in the phases of the MPCs, while the amplitudes and delays remain constant.

[2]When only single reflections are considered, an MPC with a particular arrival delay value corresponds to a reflection point that must be located somewhere on an ellipsoid around the Tx and Rx. Hence, all MPCs arriving in a particular delay interval correspond to reflection points located in a space that is bounded by two nonintersecting ellipsoids. As a result, MPCs arriving in disjoint delay intervals, correspond to reflection points located in disjoint spaces. As the positions of the reflection points form a spatial Poisson process, the numbers of reflection points in disjoint spaces are both Poisson-distributed and mutually independent, and, consequently, the numbers of MPCs in the corresponding delay intervals are also both Poisson-distributed and mutually independent.

the number of scatterers (and hence the number of MPCs) is large, it can be argued that the Poisson assumption is still a reasonable approximation when MPCs reflect upon multiple scatterers.[3]

B. Extension to the Saleh-Valenzuela Model

However, measurements suggested that MPCs have the tendency to arrive in clusters. Therefore an extension of the Poisson arrival model was suggested by Turin *et al.* [9] and developed by Suzuki [10]. In this so-called Δ-K model the homogeneous Poisson process for the MPC arrivals was replaced by a modified Poisson process, in which the MPC arrival rate temporarily changes upon the arrival of an MPC. Although the modified model turned out to describe the experimental data much more accurately, the Markov-like structure of the model made its analysis relatively complicated.

For that reason Saleh and Valenzuela introduced an alternative model [1] for indoor environments, based on a doubly stochastic Poisson process, in which the MPCs arrive in clusters. Accordingly, the expression for the complex baseband equivalent impulse response in (1) is replaced by

$$h(\tau) = \sum_{l=0}^{\infty} \sum_{k=0}^{\infty} \beta_{k,l} \, \exp(\mathrm{j}\,\phi_{k,l}) \, \delta(\tau - T_l - \tau_{k,l}) \qquad (5)$$

where $\beta_{k,l}$ and $\phi_{k,l}$ are the random amplitude and phase of the kth MPC in the lth cluster, respectively, T_l is the random arrival delay of the lth cluster (i.e., the arrival delay of the first MPC in that cluster, as $\tau_{0,l} = 0$), and $\tau_{k,l}$ is the excess arrival delay of the kth MPC in the lth cluster, measured from the start of that cluster. Both the cluster arrival delays $\{T_l\}$ and the MPC excess arrival delays $\{\tau_{k,l}\}$ are governed by homogeneous Poisson processes, with arrival rates Λ and λ, respectively. Without loss of generality, we choose $T_0 = 0$, for convenience, i.e., we ignore the absolute propagation delay between Tx and Rx.[4]

Saleh and Valenzuela attributed the arrivals in clusters to the superstructure of the building in which they performed their measurements (including large metalized walls and doors). The first cluster consists of the direct-path component and MPCs caused by the scatterers close to the Tx and Rx, while the remaining clusters consist of MPCs that are reflected off the superstructure. Assuming that the scatterers are completely randomly located, it can be argued that the arrivals in the first cluster are governed by a Poisson process, in the same way as we did for Turin's model (footnote 2). The arrival delay of each cluster corresponds to the arrival delay of the first MPC in that cluster, which is directly reflected off the superstructure. If the positions of those "superscatterers" (to be precise, the reflection points on those superscatterers) are completely randomly located, then we can apply the reasoning of footnote 2 again, and it follows that the cluster arrivals also follow a Poisson process, albeit with a lower rate. The remaining MPCs in the remaining clusters are reflected off the superstructure and additional scatterers. MPCs in the same cluster are reflected off the same superscatterer. Now suppose that the positions of the reflection points on these superscatterers (and hence the cluster arrival delays) are given. Then, even though the MPCs undergo an additional reflection upon the superscatterer, a similar reasoning[5] can be applied as for the MPCs in the first cluster, i.e., completely random distribution of the scatterers leads to excess arrival delays following Poisson processes.

An alternative explanation was suggested in the survey paper by Hashemi [11], Neyman and Scott used the spatial equivalent of the same model to describe the distribution of galaxies in space [12], [13]. Applying a similar model to the distribution of scatterers (i.e., assuming that scatterers are distributed in clusters, with cluster centers completely randomly located, and, for given cluster centers, the scatterers randomly located with density functions centered around the cluster centers), it can be argued that the arrivals of the corresponding MPCs can be approximated as a doubly stochastic Poisson process.[6]

Saleh and Valenzuela further assumed that the phases $\{\phi_{k,l}\}$ are mutually independent random variables that are uniformly distributed between 0 and 2π, and that the amplitudes $\{\beta_{k,l}\}$ are mutually independent random variables that, for given values of the arrival delays $\{T_l, \tau_{k,l}\}$, are Rayleigh-distributed, i.e.,

$$p_{\beta_{k,l}|T_l,\tau_{k,l}}(\beta) = (2\,\beta/\overline{\beta_{k,l}^2}) \exp(-\beta^2/\overline{\beta_{k,l}^2}), \quad \beta > 0 \qquad (6)$$

with conditional mean square values that are monotonically decreasing functions of T_l and $\tau_{k,l}$

$$\begin{aligned} \overline{\beta_{k,l}^2} &= \mathrm{E}\left\{\beta_{k,l}^2 | T_l, \tau_{k,l}\right\} \\ &= \overline{\beta_{0,0}^2} \, \exp(-T_l/\Gamma) \, \exp(-\tau_{k,l}/\gamma) \end{aligned} \qquad (7)$$

where $\mathrm{E}\{.\}$ denotes ensemble averaging (expected value; in this case conditioned on the values of T_l and $\tau_{k,l}$), $\overline{\beta_{0,0}^2}$ is the average energy of the first MPC in the first cluster (we will get back to this at the end of this section), and γ and Γ are the energy decay times of the individual MPCs and clusters as a whole, respectively.

The fact that (6) and (7) are conditioned on the values of T_l and $\tau_{k,l}$ means that they are only *locally valid*, as these values fluctuate with spatial position. $\overline{\beta_{k,l}^2}$ can hence be interpreted as a *local expected value* (which is not necessarily equal to the

[3]In either case, what this reasoning does not explain, is why the corresponding Poisson arrival process would be a *homogeneous* process. Considering the fact that the size of the corresponding ellipsoid increases for increasing arrival delay, one would expect that the corresponding number of interacting scatterers, and hence the arrival rate, would increase with increasing arrival delay. This would be even more pronounced when also multiple reflections are considered. On the other hand, it can reasonably be assumed that more and more scatterers get "hidden" (shadowed) as their distance from the Tx and Rx increases. The homogeneity assumption is then a convenient compromise.

[4]The physical motivation for the model is based on the assumption that the positions of the Tx and Rx are *known*, so the statistics that follow from the model are in fact conditional statistics for given distance, and, hence, given value of T_0. Therefore the additional propagation delay T_0 can always be added later in for example the expression for the PDP, by replacing τ by $\tau - T_0$.

[5]For given positions of the reflection points on the superscatterer and scatterers close to the Tx and Rx, the overall arrival delays can be found by mirroring the Rx and the scatterers close to the Rx in the plane through the reflection point on the superscatter. Consequently, for given position of the reflection point on the superscatterer, it follows from the reasoning in footnote 2 that the overall arrival delays follow a Poisson process, and the excess arrival delays follow by subtracting the cluster arrival delay (which is given for given position of the reflection point on the superscatterer).

[6]This can be argued along the same lines as in footnote 2. The resulting doubly stochastic description is only an approximation though, as the first MPC in each cluster does not correspond to a scatterer close to the center of the corresponding scatterer cluster, but to the scatterer in that cluster that is closest to the Tx and Rx.

spatial average in that area). This will be further considered in Section III.D.

The actual distributions of the amplitude and phase can be attributed to the limited measurement resolution, a large number of weak MPCs arriving shortly after each other add up to one resolvable MPC, which, through the Central Limit Theorem, has a circular complex Gaussian amplitude, and, hence, a Rayleigh-distributed amplitude and uniformly distributed phase.

Saleh and Valenzuela attributed the exponential decay of the MPC amplitudes to the fact that many MPCs result from multiple reflections, i.e., bouncing back and forth between scatterers in the vicinity of the Tx or Rx. Both the propagation delay and the attenuation in dB of such an MPC increase roughly linearly with the number of reflections (due to propagation, reflection and shadowing loss), resulting in an amplitude roughly exponentially decreasing with increasing delay.

Note that $\overline{\beta_{0,0}^2}$, the average energy of the first MPC in the first cluster, is treated as a deterministic constant here. In practice, however, it is determined by path loss and large-scale fading (shadowing), so strictly speaking it should be considered as another RV, on which (6) and (7) are conditioned, and whose value will alter upon spatial fluctuation. Although Saleh and Valenzuela do give some consideration to path loss in their paper [1], they do not consider large-scale fading. Path loss and large-scale fading will also not be incorporated in the model as it is further discussed in this paper, but we will come back to this issue in Section III.D.

III. Discussion on the Application of the Saleh–Valenzuela Model to Ultra-Wideband

As pointed out in the introduction, the SV model has also been successfully used to model UWB propagation channels, albeit with several modifications, and research aimed at the refinement of these models is still ongoing. In this section, we point out why part of the physical assumptions leading to the SV model break down when UWB channels are considered. Also we discuss spatial variation scales of the various random variables (RVs) in the model, and how the ordering of these scales changes when we extend the application of the model from WB to UWB. The latter is important for the analysis that is presented in Section IV, which further illustrates the interpretation of the SV model in a UWB context.

As will be discussed, the actual impact on the validity of the model and on the ordering of the spatial variation scales depends on whether we consider systems with a large absolute bandwidth B (UWB-ABS) or large relative bandwidth B/f_c (UWB-REL), where f_c is the center frequency [6].

A. Distortion of Individual Pulses

The most basic assumption on which the SV model was based, is Turin's hypothesis of receiving undistorted replicas of the transmitted signal, leading to the notation for the complex equivalent baseband impulse response with delta functions in (1).

Actually describing the transmitted and received signal and hence the channel itself in terms of a complex equivalent baseband representation is not compromised by increasing the bandwidth. Although this representation method was developed with narrowband signals and systems in mind, it can easily be verified that they still apply to bandpass signals and systems with ultra-large absolute or relative bandwidths, even when the lower bound of the signal frequency band approaches DC. (The only thing that is lost then is their convenient intuitive interpretation, as the envelope is no longer slowly varying compared to the carrier oscillations.)

However, what should be taken into account when UWB-REL is considered, is that the transfer functions that are experienced by individual MPCs can no longer be considered constant over the frequency band of interest, due to frequency-dependent path loss, reflections and transmissions (especially through multiple layers), diffraction, and diffuse scattering. In other words, if we maintain the (physically appealing) notation for the impulse response as in (5), where the contribution of each resolvable MPC is written as a single term in the summation, then the delta functions should be replaced by distorted pulses $\{\chi_{k,l}(\cdot)\}$, resulting in [6]

$$h(\tau) = \sum_{l=0}^{\infty} \sum_{k=0}^{\infty} \beta_{k,l}\, \chi_{k,l}(\tau - T_l - \tau_{k,l})\,. \tag{8}$$

The shapes of the complex pulses $\{\chi_{k,l}(\cdot)\}$ depend on the center frequency f_c. Considering that the transfer functions experienced by individual MPCs can only be considered constant for bandwidths much smaller than f_c (say 20% or smaller), the durations of these distorted pulses will be in the order of several times $1/f_c$ (i.e., several carrier cycles). For UWB-ABS with small relative bandwidth B/f_c this implies that the supports of the distorted pulses will be shorter than the bin duration $1/B$, so that each MPC covers only one bin, and, according to the tapped delay line model [14], might as well be described by a delta function. However, for UWB-REL, the distorted pulses might span several delay bins. Hence, if these distorted pulses were represented by delta functions using the tapped delay line model, each distorted pulse would result in several delta functions (i.e., so called phantom MPCs would be introduced). Delta functions corresponding to the same MPC would have fixed interarrival delays $(1/B)$ and mutually correlated amplitudes and phases. Hence the uncorrelated scatterers (US) assumption [15] no longer applies, and this no longer corresponds to the SV model (which assumes random interarrival delays and uncorrelated amplitudes and phases).

An additional problem is that every MPC sees a different distortion and hence has a different pulse shape $\chi_{k,l}(\cdot)$, as has recently been pointed out by Haneda *et al.* [16]. (Otherwise the effect of this frequency dependence could have been incorporated simply by convolving the expression in (5) with the common distorted pulse shape $\chi(\cdot)$, thereby completely separating the effects of multipath interference and distortion of the individual MPCs.)

B. Arrival Delay Statistics

Another important physical assumption, both in Turin's model and in the SV model, is the completely random distribution of scatterers (or more precisely, reflection points), leading to the Poisson arrivals of resolved MPCs in WB systems.

However, as the absolute bandwidth B of the system increases, the bin duration $1/B$ decreases, and more and more

individual MPCs can be resolved, with smaller and smaller interarrival delays. When the "spatial resolution" c_0/B (where c_0 is the speed of light in vacuum) becomes smaller than the sizes of some of the dominant scattering objects, many combinations of MPCs with small interarrival delays should be attributed to reflections upon the same object. This has two important consequences.

First, both the excess arrival delays and amplitudes of the MPCs can no longer be assumed independent. This is yet another reason why the US assumption breaks down (next to pulse distortion), and the MPC arrival process can no longer be assumed memoryless.

Moreover, small interarrival delays will occur relatively often (i.e., more frequently than the exponential distribution would predict). This was actually observed by Chong *et al.* [17], [18], and led to the extension from the exponential distribution for the MPC interarrival delays to a mixed-exponential distribution in the IEEE 802.15.4a models [4], [5].

In fact, at some point the notion of isolated physical MPCs and hence this way of reasoning becomes debatable, as the spatial resolution becomes so fine that the corresponding interacting objects (or parts of those objects) can no longer be considered as scattering objects. In such case one might argue that pulse broadening then becomes a matter of frequency-dependent interaction (such as diffraction), leading to the notation in (8), rather than multipath propagation. In other words, it is not possible to count the number of isolated physical MPCs in an unambiguous way.

C. Small-Scale Fading Statistics

As the absolute bandwidth and hence the number of resolvable MPCs increases, the number of physical MPCs combining to one resolvable MPC decreases. Despite the ambiguity on how to count the isolated physical MPCs (as discussed above), it is clear that, at some point, most of the remaining physical MPCs in one bin can no longer be assumed mutually independent, simply because they are scattered off the same object.

Hence the Central Limit Theorem no longer applies, so the small-scale fading statistics (i.e., around a given local mean) are no longer Rayleigh. Several alternative fading distributions (such as lognormal, Rice, Nakagami and Weibull) have been proposed. Some authors also found that the fading depth increases for increasing propagation delay [19].

D. Spatial Variation Levels of Random Variables

Apart from the arrival delay and fading statistics themselves, the way in which these statistics should be measured also changes when extending the application of the model from WB to UWB channels. This is illustrated by considering the spatial variation levels of the RVs that are involved. For simplicity, we only consider movement of the Rx, although similar reasonings can be applied to movement of the Tx and movement of the scatterers.

When the Rx moves over a distance Δd, the arrival delay of a particular MPC (resolvable or not) changes by an amount $\Delta\tau = (d/c_0)\cos\theta$, where θ is the angle between the direction of arrival of the MPC and the direction of movement of the Rx. The corresponding change in phase is $\Delta\phi = -2\pi f_c \Delta\tau$.

The amplitudes $\{\beta_{k,l}\}$ and phases $\{\phi_{k,l}\}$ of the *resolvable* MPCs are determined by the amplitudes and phases of several nonresolvable MPCs arriving in the same delay bin, which, in general, have different values of θ. Therefore, a significant change in value of the amplitudes and phases of the resolvable MPCs can be expected when $2\pi f_c \Delta d/c_0$ is the order $\pi/2$, i.e., when the spatial variation Δd is in the order of a fraction of the wavelength c_0/f_c. Hence, uncorrelated samples of the amplitude and phase can be taken by varying the position of the Tx and/or Rx on the order of the wavelength. Taking many of these samples, the local fading statistics can be estimated.

An important condition for estimating the fading statistics in this way is that the actual statistics can indeed be assumed *stationary* over these positions. In other words, the other RVs, i.e., the excess arrival delays $\{\tau_{k,l}\}$ of the resolvable MPCs, the cluster arrival delays $\{T_l\}$, and $\overline{\beta_{0,0}^2}$, the average energy of the first MPC in the first cluster, should all be constant in that area.

First of all, this requires the path loss and large-scale fading to be more or less constant. The corresponding restriction to the spatial variation scale depends on the frequency and the distance between the Tx and Rx, but not really on the considered bandwidth, so we do not further consider this here.[7]

The situation is different for changes in excess arrival delays $\{\tau_{k,l}\}$ of the resolvable MPCs. These can be considered significant when they are in the order of the bin duration $1/B$ or more; this would result in MPCs moving from one bin to the other, leading to a change in the fading statistics. From the above it follows that this occurs when the spatial variation Δd is in the order of c_0/B or more.[8]

Hence it can be concluded that the amplitudes and phases can be assumed significantly different while still satisfying the same conditional statistics, if the spatial variation is more than a fraction of the wavelength c_0/f_c but less than c_0/B. Note that this is only possible for small relative bandwidths B/f_c. For UWB-REL, the two spatial variation levels can no longer be clearly separated. The interpretation of this phenomenon and its influence on the collection of channel parameters will be considered in further detail in Section IV.H.

From (4) it follows that the mean and standard deviation of the interarrival delays are both equal to $1/\lambda$. In that sense, it takes displacements in the order of several times c_0/λ (which is larger than c_0/B for sparse channels) before the MPC excess arrival delays can be considered as RVs that are governed by (3) and (4).

[7]Assuming that at least the *shape* of the fading distribution (for instance Rayleigh or Nakagami) can be assumed consistent over a larger area, and that only parameters such as the mean square amplitude change from one local area to the other, the fading statistics collected over several local areas can be combined by applying the proper normalization [20]. However, in this paper we only consider how to interpret the conditional statistics as local statistics; whether these local statistics can be generalized to statistics describing the complete environment is considered outside the scope of this paper.

[8]Two sidenotes should be made here. First, in fact only the MPCs coming in along (or opposite to) the direction of movement will move significantly. Second, the tapped delay line model is only an approximation; if the MPC does not arrive in the center of a bin, there is spill-over of energy in adjacent bins, which increases as the MPC moves towards the border of the bin. Hence MPCs do not really "hop" from one bin to another, but rather move gradually. The main point remains valid though: fading statistics can be considered constant for spatial variations much smaller than c_0/B, and they change significantly for spatial variations larger than c_0/B.

TABLE I
SV MODEL PARAMETERS VALUES USED IN THE EXAMPLES IN THIS PAPER (FROM [1])

parameter	symbol	value	unit
cluster arrival rate	Λ	1/300	ns^{-1}
cluster energy decay time	Γ	60	ns
MPC arrival rate	λ	1/5	ns^{-1}
MPC energy decay time	γ	20	ns

Basically the same spatial variation scale applies to the MPC excess arrival delays $\{\tau_{k,l}\}$ and cluster arrival delays $\{T_l\}$. The arrival delay of the first MPC in a cluster is equal to the arrival delay of that cluster, so when the Rx moves over a distance c_0/B towards a cluster of scatterers (or towards a superscatterer), the arrival delay of the corresponding cluster of MPCs will change by one bin duration $1/B$, and can be considered significant. A (somewhat artificial) distinction can be made between the spatial separation scales when we consider *dense channels*, i.e., channels with MPC arrival rate λ that is much larger than the bandwidth B, so that the mean number of MPC arrivals per bin (λ/B) is high, and their relative variation is low. In other words, individual MPC arrivals (and hence changes in their arrival delays) are no longer visible in the PDP (we will consider this in more detail in Section IV.E), but the clusters are visible as envelopes with duration γ. From this perspective, changes in the cluster arrival delays can be considered insignificant when they are smaller then γ, i.e., for spatial variations smaller than $c_0\gamma$. The mean and standard deviation of the cluster interarrival delays are equal to $1/\Lambda$, so in that sense, changes in the cluster arrival delays can be considered significant for spatial variations on the order of several times c_0/Λ.

IV. POWER DELAY PROFILES OF THE SALEH-VALENZUELA MODEL

In this section analytical expressions for the average PDP and related channel properties will be provided for different levels of the ensemble averaging, based on the classical SV model described in Section II.B and spatial variation levels discussed in Section III.D. These expressions will be illustrated by numerical examples based on the original parameter values that Saleh and Valenzuela found [1], which are given in Table I.

As a matter of fact, several analyses on different versions of the SV model can be found in literature (among others [21]) based on more general versions of the model and more sophisticated mathematical tools than we will present here. The main purpose of the analytical results presented in this section is to establish a clear definition of the different ensemble averaging levels, and to discuss their physical interpretation as local channel properties, linking them to the spatial variation scales discussed in Section III.D. We limit mathematical rigor, and base our analysis on the simplest possible version of the model.[9] As discussed in Section III.D, the notion of the different averaging levels and their corresponding spatial ergodicity is especially important when we consider the extension to UWB-REL channels, and helps to illustrate some fundamental differences between the characterization of UWB-ABS channels and UWB-REL channels.

The analysis will initially be based on the assumption of low relative bandwidths (UWB-ABS), so that the notation with delta functions in (5) can be used, and the spatial variation scales for small-scale fading and arrival delays can be clearly separated. We start with the definition of the PDP and some related channel properties, and then derive analytical expressions for the cases in which these properties are averaged over small-scale fading, the MPC excess arrival delays and the cluster excess arrival delays, respectively. Then we discuss the case in which these properties are also averaged over the absolute arrival delay T_0, i.e., the arrival delay of the very first MPC. Finally, we consider the case of UWB-REL, where the notation with the delta functions breaks down and the spatial variation levels of small-scale fading and arrival delays can no longer be separated.

A. Definition of Power Delay Profile

The PDP specifies the power (energy density) of a signal received through a multipath channel as a function of delay [14]. For a finite-valued impulse response $h(\tau)$ (i.e., in case of a band-limited transfer function), this can be described by $|h(\tau)|^2$, since the received power $|y(t)|^2$ as a function of time t is equal to $|h(t)|^2$ when the transmitted signal $x(t)$ is equal to a delta function $\delta(t)$. In measurements this bandwidth limitation is either intrinsic to the hardware that is involved, or to the processing that is performed (for instance because the inverse FFT of the transfer function measured over a limited frequency window is taken). The "average PDP" is then measured by spatially averaging the measured $|h(\tau)|^2$ over an appropriate local area.[10] The analytical equivalent (i.e., ensemble-averaged PDP) is given by

$$P_h(\tau) = \mathrm{E}\left\{|h(\tau)|^2\right\} = R_h(\tau,\tau) \tag{9}$$

where $R_h(\cdot,\cdot)$ is the autocorrelation function of $h(\tau)$

$$R_h(\tau,\tau') = \mathrm{E}\left\{h^*(\tau)h(\tau')\right\}\ . \tag{10}$$

In case of the SV model, $h(\tau)$ is given by (5) and the autocorrelation function becomes

$$R_h(\tau,\tau') = \sum_{l=0}^{\infty}\sum_{l'=0}^{\infty}\sum_{k=0}^{\infty}\sum_{k'=0}^{\infty}\mathrm{E}\left\{\beta_{k,l}\beta_{k',l'}\exp(-\mathrm{j}\,\phi_{k,l})\right.$$
$$\left.\cdot\exp(\mathrm{j}\,\phi_{k',l'})\,\delta(\tau - T_l - \tau_{k,l})\,\delta(\tau' - T_{l'} - \tau_{k',l'})\right\}\ . \tag{11}$$

Note that the impulse response (5) is written as a sum of delta functions, so it is not band-limited. Defining the PDP as in (9) would hence introduce a singularity problem; the resulting PDP would contain squared delta functions, so it would not be possible to derive for instance mean delay or delay spread from it. The common way to overcome this analytical inconvenience in case of a wide-sense stationary uncorrelated scatterers (WSSUS) channel [15] is by defining the PDP in a different way, namely by writing the autocorrelation function as [14]

$$R_h(\tau,\tau') = P_h(\tau)\,\delta(\tau - \tau') \tag{12}$$

[9]Note that our aim is to illustrate the notion of the different averaging levels and spatial variation levels, rather than to give an accurate prediction of what could be measured in practice.

[10]What should be considered an appropriate local area will be discussed in Sections IV.C– IV.H.

where $P_h(\tau)$ is the delay cross power spectral density, which, in case of a static channel, is denoted as PDP, even though that is not consistent with (9). (It can be verified that $P_h(t)$ then represents the instantaneous received power $|y(t)|^2$ as a function of time t when the instantaneous power $|x(t)|^2$ of the transmitted signal $x(t)$ is equal to a delta function $\delta(t)$.)

In our case we can write (11) in the form of (12) by assuming that, upon taking the expected value, the phases $\{\phi_{k,l}\}$ are treated as independent uniformly distributed RVs, so that only the terms with $k = k'$ and $l = l'$ remain, resulting in

$$P_h(\tau) = \sum_{l=0}^{\infty} \sum_{k=0}^{\infty} \mathrm{E}\left\{\beta_{k,l}^2 \delta(\tau - T_l - \tau_{k,l})\right\} . \tag{13}$$

Note, however, that implementing the WSSUS assumption in this way in fact already involves averaging over the phases. Although this is indeed the appropriate first averaging step for UWB-ABS (because the small-scale fading has the smallest spatial scale of variation, as was discussed in Section III.D and will be further discussed in Section IV.D), we should strictly speaking also average over the amplitudes (i.e., substitute (7) into (13)) to complete the averaging over the small-scale fading. Nevertheless, we can justify dropping the terms with $k \neq k'$ or $l \neq l'$ by noting that these denote the cross terms between different MPCs; these do not appear in the PDP for fixed values of the arrival delays, simply because these values are all different, and the delta functions have zero duration.[11]

As a result, we find that the autocorrelation function of the channel impulse response is equal to the sum of the autocorrelation functions of the individual MPCs (the cross correlation functions are zero), and the expression within the braces in (13) denotes the PDP *before* doing any averaging. The evaluation of the ensemble average depends on the RVs over which the averaging is performed, and can be expressed in the contributions of the individual clusters by writing

$$P_h(\tau) = \sum_{l=0}^{\infty} \mathrm{E}\left\{P_l(\tau - T_l)\right\} \tag{14}$$

where

$$P_l(\tau) = \sum_{k=0}^{\infty} \mathrm{E}\left\{\beta_{k,l}^2 \delta(\tau - \tau_{k,l})\right\} \tag{15}$$

is the PDP per cluster. The averaging in (15) depends on the RVs over which the averaging is performed, but does not include possible averaging over the cluster arrival delays $\{T_l\}$; that averaging step should be taken only after substitution in (14) (and is then the only remaining averaging step).

B. Additional Channel Properties

The channel impulse response can also be described in more condensed parameters, that follow from the moments of the PDP. The mean power gain $\bar{G}$, the mean excess delay $\bar{\tau}$ and RMS delay spread σ_τ can be derived from the PDP as [14]

$$\bar{G} = \int_{-\infty}^{\infty} P_h(\tau)\,\mathrm{d}\tau \tag{16}$$

$$\bar{\tau} = \frac{1}{\bar{G}} \int_{-\infty}^{\infty} \tau\, P_h(\tau)\,\mathrm{d}\tau \tag{17}$$

$$\sigma_\tau^2 = \frac{1}{\bar{G}} \int_{-\infty}^{\infty} (\tau - \bar{\tau})^2 P_h(\tau)\,\mathrm{d}\tau. \tag{18}$$

For a WSSUS channel the frequency correlation function (FCF), which is the autocorrelation of the transfer function $H(f)$, only depends on the frequency difference Δf, and is given by the Fourier transform of the PDP [14][12]

$$\begin{aligned} R_H(\Delta f) &= \mathrm{E}\left\{H^*(f) H(f + \Delta f)\right\} \\ &= \int_{-\infty}^{\infty} P_h(\tau) \exp(-\mathrm{j}\, 2\pi \Delta f\, \tau)\,\mathrm{d}\tau\,. \end{aligned} \tag{19}$$

In terms of the notation in (14) and (15), these become

$$\bar{G} = \sum_{l=0}^{\infty} \mathrm{E}\{\bar{G}_l\} \tag{20}$$

$$\bar{\tau} = \frac{1}{\bar{G}} \sum_{l=0}^{\infty} \mathrm{E}\left\{\bar{G}_l (T_l + \bar{\tau}_l)\right\} \tag{21}$$

$$\sigma_\tau^2 = \frac{1}{\bar{G}} \sum_{l=0}^{\infty} \mathrm{E}\left\{\bar{G}_l \left[\sigma_{\tau,l}^2 + (T_l + \bar{\tau}_l)^2\right]\right\} - \bar{\tau}^2 \tag{22}$$

$$R_H(\Delta f) = \sum_{l=0}^{\infty} \mathrm{E}\left\{R_l(\Delta f) \exp(-\mathrm{j}\, 2\pi \Delta f\, T_l)\right\} \tag{23}$$

where

$$\bar{G}_l = \int_{-\infty}^{\infty} P_l(\tau)\,\mathrm{d}\tau = \sum_{k=0}^{\infty} \mathrm{E}\left\{\beta_{k,l}^2\right\} \tag{24}$$

$$\bar{\tau}_l = \frac{1}{\bar{G}_l} \int_{-\infty}^{\infty} \tau\, P_l(\tau)\,\mathrm{d}\tau = \frac{1}{\bar{G}_l} \sum_{k=0}^{\infty} \mathrm{E}\left\{\beta_{k,l}^2 \tau_{k,l}\right\} \tag{25}$$

$$\begin{aligned} \sigma_{\tau,l}^2 &= \frac{1}{\bar{G}_l} \int_{-\infty}^{\infty} (\tau - \bar{\tau}_l)^2 P_l(\tau)\,\mathrm{d}\tau \\ &= \frac{1}{\bar{G}_l} \sum_{k=0}^{\infty} \mathrm{E}\left\{\beta_{k,l}^2 (\tau_{k,l} - \bar{\tau}_l)^2\right\} \end{aligned} \tag{26}$$

$$\begin{aligned} R_l(\Delta f) &= \int_{-\infty}^{\infty} P_l(\tau) \exp(-\mathrm{j}\, 2\pi \Delta f\, \tau)\,\mathrm{d}\tau \\ &= \sum_{k=0}^{\infty} \mathrm{E}\left\{\beta_{k,l}^2 \exp(-\mathrm{j}\, 2\pi \Delta f\, \tau_{k,l})\right\} \end{aligned} \tag{27}$$

are the corresponding properties *per cluster*. Again, the evaluation of all these channel properties depends on the RVs over which the ensemble averaging is performed, and the averaging

[11] As Saleh and Valenzuela already pointed out [1], the overlap between MPCs does become relevant in case of transmitted pulses with finite durations in the same order as differences between the arrival delays. They solved this issue in their measurements by sweeping the carrier frequency of their pulses and averaging the measured PDP over the sweeping window. Hence they could resolve paths that were separated by delays at least as large as the inverse of the window width.

[12] Note that the FCF is fundamentally different from the second-order power spectral characteristics that are derived in [22] and [23]; the latter concern the (normalized) autocovariance function of the power transfer $|H(f)|^2$, whereas the FCF is the autocorrelation of the transfer function $H(f)$ itself. Relating them is far from straightforward due to the complicated underlying statistics of $H(f)$. Since the (complex) FCF is the most general of the two (it describes both the power and phase transfer) and has a very simple relation to the PDP, we only consider the FCF here.

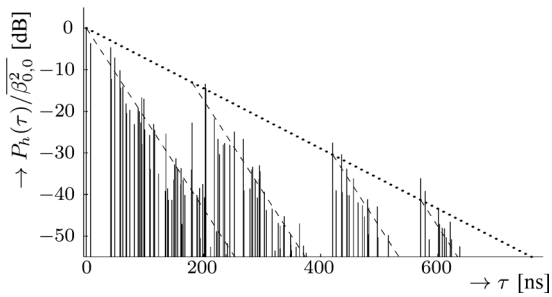

Fig. 1. Example of an analytical PDP for a given channel realization, normalized to the expected energy of the first MPC. The positions and heights of the vertical lines correspond to the arrival delays and normalized energies of the MPCs, the dashed lines represent the exponential decay of the average MPC energy in each cluster, and the dotted line represents the exponential decay of the average cluster energy.

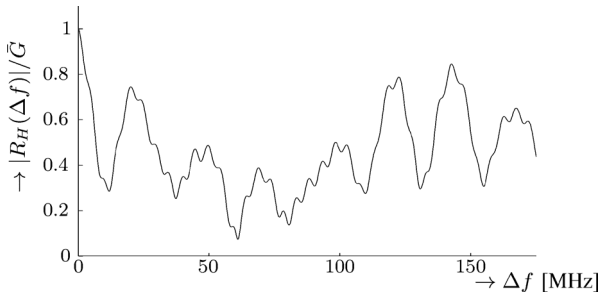

Fig. 2. Example of the magnitude of an analytical FCF for a given channel realization, normalized to the overall power gain.

in the properties per cluster does not include the averaging over the cluster arrival delays $\{T_l\}$.

C. Channel Properties for Known Values of the Channel Variables

Initially we consider the scenario in which we assume that the positions of Tx, Rx and scatterers are fixed, and that the values of all channel variables $\{\beta_{k,l}, \tau_{k,l}, T_l\}$ are *known* (for instance using estimation strategies based on knowledge of the model structure [7]). The PDP, mean channel gain, mean delay, RMS delay spread, and FCF then follow by simply substituting these values in (14), (15), and (20) through (27), without doing any averaging.

As a numerical example, a simulation was run in Matlab in which these parameter values were generated according to the probability distributions specified in Section II.B and the model parameters specified in Table I. The resulting PDP is normalized to the expected energy $\overline{\beta_{0,0}^2}$ of the first MPC, and plotted in Fig. 1. The clusters of MPCs starting at $T_0 = 0$, $T_1 = 180$ ns, $T_2 = 421$ ns and $T_4 = 571$ ns are clearly visible. The energies of the first MPC in each cluster roughly follow the exponential envelope indicated by the dotted line, while the remaining MPCs in each cluster roughly follow the exponential envelopes indicated by the dashed lines. The fluctuation around the envelopes is due to the Rayleigh fading. The total power gain $\bar{G}$ is 2.5 times the expected energy of the first MPC, the mean excess delay $\bar{\tau}$ is 32 ns, and the RMS delay spread σ_τ is 52 ns.

The magnitude of the corresponding FCF is normalized to $\bar{G}$ and plotted as a function of the frequency difference Δf in Fig. 2. An important observation here is that the FCF purely consists of complex harmonic terms due to the *known* values of the arrival delays $\{\tau_{k,l}, T_l\}$. Therefore the FCF does not decay to zero for large values of Δf. In this case the shape of the FCF is strongly influenced by the dominating first three MPCs in the PDP, which occur at $T_0 + \tau_{0,0} = 0$, $T_0 + \tau_{1,0} = 7$ ns, and $T_0 + \tau_{2,0} = 42$ ns, introducing strong harmonic terms in the FCF with periods $1/\tau_{1,0} = 140$ MHz and $1/\tau_{2,0} = 24$ MHz, respectively.

Note that the PDP and FCF were calculated and plotted without considering that the bandwidth B will be limited in general. In practice, the contribution of individual MPCs will have a finite duration because of this bandwidth limitation. Moreover, two MPCs might have a delay difference that is too small to resolve them. With a tapped delay line model in mind, this means that the MPCs arrive in the same delay bin (with duration $1/B$), and, as result, will interfere, leading to one resolvable MPC with a total energy that depends on the phase difference between the two MPCs. The WSSUS assumption is no longer satisfied, so the measured FCF will depend not only on the frequency difference Δf, but also on the absolute frequency f. (In fact the derived expression will only be valid for absolute frequencies below the bandwidth.)

D. Channel Properties Averaged Over Small-Scale Fading

A more common way to define the PDP is to average over the small-scale fading, i.e., over the random amplitudes $\{\beta_{k,l}\}$. This results in the PDP for given (known) values of the cluster arrival delays $\{T_l\}$ and MPC excess arrival delays $\{\tau_{k,l}\}$. As discussed in Section III.D, this physically makes sense for UWB-ABS, because the amplitudes then rapidly change with displacement of Tx, Rx or scatterers, while it takes larger displacement to note significant changes in the arrival delays of the MPCs and clusters; as long as the relative bandwidth B/f_c is small, spatial variations on the order of a wavelength will change the fading amplitudes (i.e., the difference in height between the peaks and the envelopes in Fig. 1) but not the arrival delays (the positions of the peaks and envelopes in Fig. 1). This suggests that the corresponding average PDP can then be measured by averaging over a spatial grid of several wavelengths wide, and it can be used to identify the MPCs and study their arrival delays.

The corresponding analytical results are given by (14) and (20)–(23), where the averaged properties per cluster can be found by substituting (7) in (15) and (24)–(27), resulting in

$$P_l(\tau) = \overline{\beta_{0,l}^2} \exp(-\tau/\gamma) \sum_{k=0}^{\infty} \delta(\tau - \tau_{k,l}) \tag{28}$$

$$\bar{G}_l = \overline{\beta_{0,l}^2} \sum_{k=0}^{\infty} \exp(-\tau_{k,l}/\gamma) \tag{29}$$

$$\bar{\tau}_l = \frac{\overline{\beta_{0,l}^2}}{\bar{G}_l} \sum_{k=0}^{\infty} \tau_{k,l} \exp(-\tau_{k,l}/\gamma) \tag{30}$$

$$\sigma_{\tau,l}^2 = \frac{\overline{\beta_{0,l}^2}}{\bar{G}_l} \sum_{k=0}^{\infty} (\tau_{k,l} - \bar{\tau}_l)^2 \exp(-\tau_{k,l}/\gamma) \tag{31}$$

$$R_l(\Delta f) = \overline{\beta_{0,l}^2} \sum_{k=0}^{\infty} \exp(-\tau_{k,l}/\gamma - \mathrm{j}\, 2\pi \Delta f\, \tau_{k,l}) \tag{32}$$

where $\overline{\beta_{0,l}^2} = \overline{\beta_{0,0}^2} \exp(-T_l/\Gamma)$.

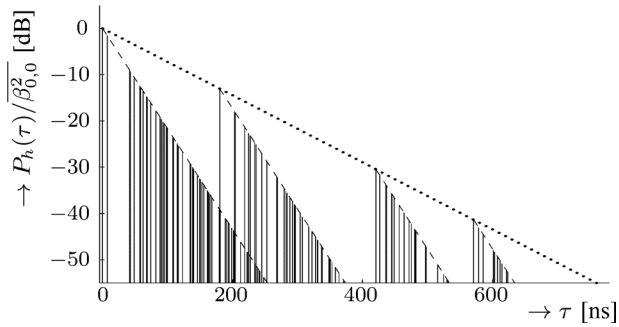

Fig. 3. Example of an analytical PDP for given MPC and cluster arrival delays (i.e., averaged over small-scale fading), normalized to the expected energy of the first MPC. The positions and heights of the vertical lines correspond to the arrival delays and normalized average energies of the MPCs, the dashed lines represent the exponential decay of the average MPC energy in each cluster, and the dotted line represents the exponential decay of the average cluster energy.

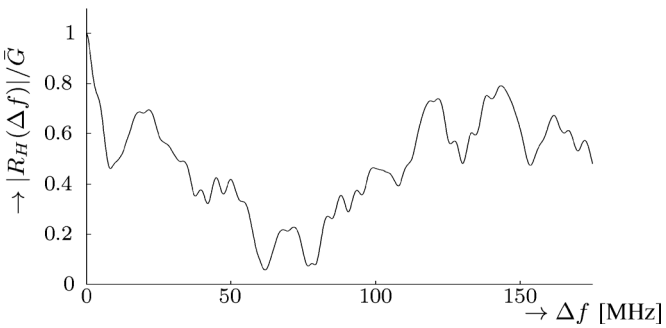

Fig. 4. Example of an analytical FCF for given MPC and cluster arrival delays (i.e., averaged over small-scale fading), normalized to the mean overall power gain.

As a numerical example, the variables that were generated in the previous subsection were substituted in the equations above, (14), and (20) through (23) (i.e., no new simulation was run). The resulting normalized PDP and FCF are plotted in Figs. 3 and 4, respectively. The energies of the MPCs now clearly follow the exponential envelopes; the effect of fading has been averaged out. The total power gain is now 2.6 times the expected energy of the first MPC, the mean excess delay is 30 ns, and the RMS delay spread is 52 ns. Note that the third MPC in Fig. 3 has become less significant due to the averaging, so that the harmonic term with period of 24 MHz has become almost invisible in Fig. 4.

The same considerations for bandwidth limitation apply as for the previous numerical example. The only difference is that the average energies of MPCs in the same bin now simply add up, as the effect of the random phase difference has been averaged out.

Another aspect to reconsider here is the physical motivation for the exponential envelopes that we gave at the end of Section II.B. In order to randomize the actual losses described there (and hence achieve a spatial average approaching the exponential envelopes derived above), variations over a spatial scale larger than the wavelength are required, but this would also randomize the arrival delays. We will come back to this ergodicity issue in the next subsection, but this already shows that spatially averaging measured PDPs is not likely to result in an average PDP containing individual MPCs spanning only one delay bin while following perfectly exponential envelopes (as in Fig. 3).

E. Channel Properties Averaged Over Small-Scale Fading and MPC Excess Arrival Delays

For larger displacements (in the order of c_0/B) the MPC excess arrival delays $\{\tau_{k,l}\}$ will also start to vary significantly and should also be treated as unknowns. For displacements as large as several times c_0/λ, we can consider them as RVs that are governed by (3) and (4). As discussed in Section III.D, this strictly speaking implies that the arrival delay of the first MPC in each cluster, and hence the cluster arrivals delays $\{T_l\}$, should also be treated as unknowns, but we consider these as known and fixed for the moment (albeit a bit artificial). We will come back to this later.

The MPC arrivals in the clusters can now be considered as homogeneous Poisson processes with known starting times $\{T_l\}$, so the overall arrival process can be considered as an inhomogeneous Poisson process with an arrival rate that increases in steps, at known delay instants $\{T_l\}$

$$\lambda(\tau) = \sum_{l=0}^{\infty} \lambda_l(\tau - T_l), \text{ with } \lambda_l(\tau) = \delta(\tau) + \lambda\, \mathrm{u}(\tau) \quad (33)$$

where $\mathrm{u}(\,\cdot\,)$ is the unit step function. The unit-area delta functions indicate the certain arrival of the first MPC in each cluster at known arrival delay T_l, while the step functions indicate homogeneous Poisson arrivals of the remaining MPCs in each cluster. The occurrence of the delta function can be debated as it exactly marks the discrepancy noted earlier; if the excess arrival delays of the remaining MPCs are not known precisely, then the arrival of the first MPC in each cluster will also not be known precisely. We will come back to this again after the derivation of the average channel properties.

The average PDP follows by averaging (28) over the MPC excess arrival delays $\{\tau_{k,l}\}$, using (3) and (4). Likewise, the expected values over the summations in (29) through (32) can be found, leading to the other averaged channel properties. Alternatively, Campbell's theorem can be applied [21], as the individual clusters govern homogeneous Poisson processes. Either way, the results are given by

$$P_l(\tau) = \overline{\beta_{0,l}^2}\,[\delta(\tau) + \lambda\, \mathrm{u}(\tau) \exp(-\tau/\gamma)] \quad (34)$$

$$\bar{G}_l = \overline{\beta_{0,l}^2}(1 + \lambda\,\gamma) \quad (35)$$

$$\bar{\tau}_l = \gamma \left(1 - \frac{1}{1 + \lambda\,\gamma}\right) \quad (36)$$

$$\sigma_{\tau,l}^2 = \gamma^2 \left[1 - \left(\frac{1}{1 + \lambda\,\gamma}\right)^2\right] \quad (37)$$

$$R_l(\Delta f) = \overline{\beta_{0,l}^2} \left(1 + \frac{\lambda\,\gamma}{1 + \mathrm{j}\,2\pi\Delta f\,\gamma}\right). \quad (38)$$

As a numerical example, the parameter values that were obtained in the previous two subsections were substituted in the equations above. The resulting normalized PDP and FCF are plotted in Figs. 5 and 6, respectively. The total power gain $\bar{G}$ is now 5.3 times the expected energy of the first MPC, the mean excess delay $\bar{\tau}$ is 25 ns, and the RMS delay spread σ_τ is 45 ns. (The lower values of $\bar{G}$ and higher values for $\bar{\tau}$ and σ_τ in the

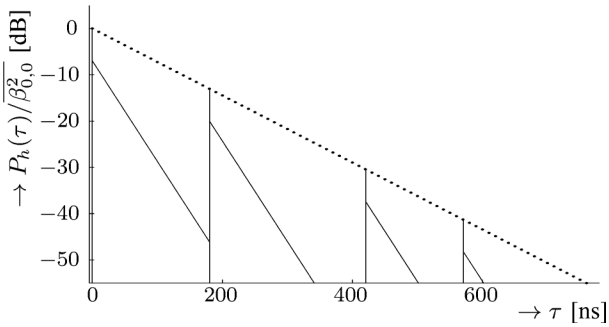

Fig. 5. Example of an analytical PDP for given cluster arrival delays (i.e., averaged over small-scale fading and MPC arrival delays), normalized to the expected energy of the first MPC. The positions and heights of the vertical lines correspond to the arrival delays and normalized average energies of the first MPC in each cluster, the tilted solid lines represent the average PDP due to the remaining MPCs in the clusters, and the dotted line represents the exponential decay of the average cluster energy.

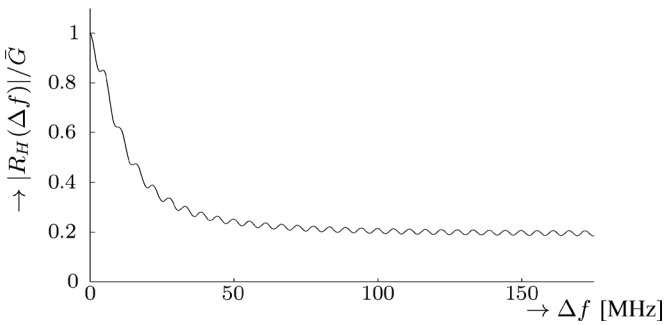

Fig. 6. Example of an analytical FCF for given cluster arrival delays (i.e., averaged over small-scale fading and MPC arrival delays), normalized to the mean overall power gain.

previous examples should be attributed to the relatively late arrivals of MPCs in the first cluster.)

Obviously, for known cluster arrival delays, the average PDP consists of cluster contributions with consistent shapes (and hence consistent values for the mean excess delay and RMS delay spread per cluster). Each cluster contribution consists of one discrete contribution, corresponding to the first MPC with the known arrival delay, and an exponential continuous contribution, corresponding to the exponential envelope of the remaining MPC amplitudes.

Again, the occurrence of the delta function can be debated here. As discussed in Section III.D, introducing a spatial variation that is sufficient for randomizing the MPC arrival delays, would also blur the knowledge of the precise arrival delay of the cluster. Since the model is based on the assumption that the start of the cluster is marked by the arrival of the first MPC in that cluster, exact knowledge of the arrival delay of a cluster implies exact knowledge of the arrival delay of that first MPC. Therefore, the above-mentioned discrepancy in our interpretation of the model could be removed by making a slight change to the model, namely by simply removing the first MPC in each cluster. In other words, we start counting from $k = 1$ instead of $k = 0$ in (5), so that the excess arrival delay of the first MPC in each cluster becomes $\tau_{1,l}$, which is Poisson-distributed instead of known. As Saleh and Valenzuela pointed out, this hardly makes a difference to the overall model when $\lambda\gamma \gg 1$; the number of significant MPCs is then so large that it is hardly changed by removing the first MPC in each cluster, and the statistical behavior of the *total* arrival delay $T_l + \tau_{k,l}$ of the remaining MPCs stays roughly the same. Besides the convenience this brings in the way we interpret the model (where conditional statistics are interpreted as local statistics), the analytical results also become a lot simpler; the delta functions in the cluster arrival rate $\lambda_l(\tau)$ and cluster PDP $P_l(\tau)$ disappear, the horizontal asymptote in the cluster FCF $R_l(\Delta f)$ disappears (we will come back to this later), and the average gain, mean excess delay and RMS delay spread per cluster are then simply given by $\bar{G}_l = \overline{\beta_{0,l}^2}\,\lambda\gamma$ and $\bar{\tau}_l = \sigma_{\tau,l} = \gamma$.[13] On the other hand, one could advocate that at least the arrival delay of the first MPC in the first cluster (with $k = l = 0$) remains known upon spatial fluctuation, assuming that the Rx remains synchronized to the Tx. (We will come back to this in Section IV.G.) With this assumption the MPCs with $k = 0$ should be omitted in all clusters except the first (with $l = 0$). Nevertheless, for completeness, we proceed our discussion here with the model including the MPCs with $k = 0$ in all clusters.

The correspondence between the exponential parts of the PDP in (34) and the exponential envelopes of the MPC amplitudes in (28) immediately follows from Campbell's Theorem and the fact that the individual arrival processes for the different clusters are all homogeneous [21]. It can also be found from the following interesting interpretation. By averaging over the excess arrival delays, the delta functions in (28) are basically replaced by the corresponding probability density functions of $\tau_{k,l}$, which are Erlang for $k \geq 1$

$$p_{\tau_{k,l}}(\tau) = \mathrm{u}(\tau)\exp(-\lambda\tau)\frac{\lambda^k\tau^{k-1}}{(k-1)!}\,. \tag{39}$$

(For $k = 0$, we have $\tau_{k,l} = 0$ so $p_{\tau_{0,l}}(\tau) = \delta(\tau)$.) Hence, the individual MPCs (except the first in each cluster) are delay-dispersed due to the averaging, with increasing dispersion for later MPCs. It can be shown that the contributions of the individual MPCs in a cluster sum up to the rate function per cluster in (33), i.e.,

$$\sum_{k=0}^{\infty} p_{\tau_{k,l}}(\tau) = \lambda_l(\tau)\,. \tag{40}$$

The resulting cluster PDPs hence have the same shape as the exponential envelope in (28).[14]

Due to the consistent and gradual shape of the PDP per cluster, the FCF now has a much smaller width, in the order of $1/(2\pi\gamma) = 8$ MHz. It still does not decay to zero for large values of Δf; there is a horizontal asymptote due to the known arrival delays of the first MPCs in each cluster, most notably the first one. As argued before, the latter makes sense with the assumption that the Rx remains synchronized to the Tx upon spatial fluctuation. We will come back to this in Section IV.G. The small ripple is caused by the known arrival delay of the

[13]This is probably the reason why this modified version of the model has already appeared in literature numerous times.

[14]It can be shown that this is not the case when for example a mixed exponential distribution is assumed for the MPC interarrival delays, as is done in the IEEE 802.15.4a models [4], [5].

(low-energy) second cluster, resulting in a ripple period of $1/T_1 = 5.5$ MHz.

Note that a bandwidth limitation would now hardly affect the shape of the PDP (except for the delta functions), because the exponential functions already have a gradual shape. This is exactly why this is a very common averaging level to describe the PDP in case there is insufficient resolution to see individual MPCs, i.e., delay bins of width $1/B$ typically contain more than one MPC. However, in general the number of arrivals per bin will be random due to the random arrival delays, so the measured PDP would not follow the exponential envelope (unless the channel were dense, i.e., the arrival rate λ were much larger than the bandwidth B, but then there would be no point in explicitly modeling the arrival delays of the individual MPCs).

Also note that the result represents the *expected* channel properties, i.e., the channel properties that can be expected to be measured when the positions of the Tx and/or Rx are varied over distances in the order of c_0/λ. This will not necessarily be equal to the *average* properties that are indeed obtained by averaging the results that are acquired at the individual positions in that local area. This follows from the following geometrical consideration.

- When the Tx or Rx is directly surrounded by the scatterers corresponding to the MPCs that are considered, varying its position will change the directions of the incoming MPCs, randomizing the fluctuation of their arrival delays.
- However, when a cluster of scatterers somewhat further away from the Tx and Rx is considered, fluctuating the positions of the Tx and Rx will hardly change the directions of the incoming MPCs, and hence the differences between the arrival delays will hardly change.

In other words, the impulse response of the channel as a function of the Tx/Rx position cannot be considered as a *spatially ergodic* process, even when its statistics can be considered stationary in that area. An important consequence of this notion is that the expected channel properties and statistics of the MPC arrival delays for given values of the cluster arrival delays can in general (especially for later clusters) *not* be obtained simply by varying the positions of the Tx and/or Rx; the positions of the relevant scatterers would need to be varied as well. Alternatively, the statistics can be collected by considering a larger area, but then the acquisition is complicated by the fact that the statistics might no longer be considered stationary in that area.

F. Channel Properties Averaged Over All Random Variables

For even larger displacements (i.e., in the order of $c_0\gamma$ or larger), the variations in the cluster arrival delays $\{T_l\}$ also become significant, so these could also be treated as (unknown) RVs. Considering them as a Poisson sequence results in an overall MPC arrival process with intensity function [21]

$$\lambda(\tau) = \delta(\tau) + (\lambda + \Lambda + \lambda\,\Lambda\,\tau)\,\mathrm{u}(\tau)\,. \tag{41}$$

The expected PDP and other channel properties can then be found by substituting the results of the previous subsection in (20) through (23), and averaging over the cluster arrival delays $\{T_l\}$ in the same way as we averaged over the MPC excess arrival delays $\{\tau_{k,l}\}$ in the previous subsection, resulting in

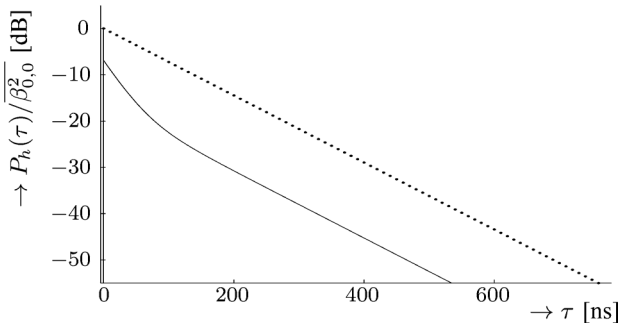

Fig. 7. Example of an analytical PDP averaged over all random variables (small-scale fading and all arrival delays), normalized to the expected energy of the first MPC. The position and height of the vertical line corresponds to the arrival delay and normalized average energy of the first MPC, the tilted solid line represents the average PDP due to the remaining MPCs, and the dotted line represents the exponential decay of the average cluster energy.

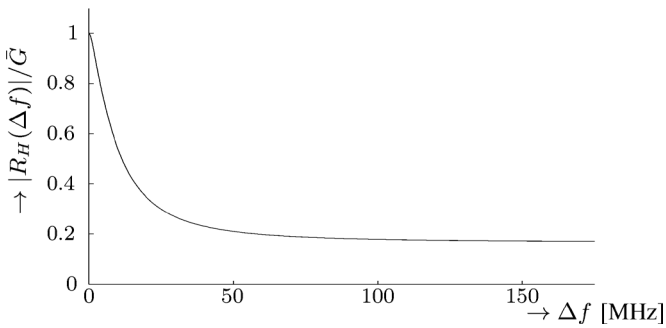

Fig. 8. Example of an analytical FCF averaged over all random variables (small-scale fading and all arrival delays), normalized to the mean overall power gain.

$$P_h(\tau) = \overline{\beta_{0,0}^2}\left[\delta(\tau) + \lambda\left(1 - \frac{\gamma\,\Lambda\,\Gamma}{\Gamma - \gamma}\right)\exp(-\tau/\gamma) + \Lambda\left(1 + \frac{\lambda\,\gamma\,\Gamma}{\Gamma - \gamma}\right)\exp(-\tau/\Gamma)\right] \tag{42}$$

$$\bar{G} = \overline{\beta_{0,0}^2}(1 + \lambda\,\gamma)(1 + \Lambda\,\Gamma) \tag{43}$$

$$\bar{\tau} = \bar{\tau}_l + \Gamma\left(1 - \frac{1}{1 + \Lambda\,\Gamma}\right) \tag{44}$$

$$\sigma_\tau^2 = \sigma_{\tau,l}^2 + \Gamma^2\left[1 - \left(\frac{1}{1 + \Lambda\,\Gamma}\right)^2\right] \tag{45}$$

$$R_H(\Delta f) = \overline{\beta_{0,0}^2}\left(1 + \frac{\lambda\,\gamma}{1 + \mathrm{j}2\pi\Delta f\,\gamma}\right) \cdot \left(1 + \frac{\Lambda\,\Gamma}{1 + \mathrm{j}2\pi\Delta f\,\Gamma}\right)\,. \tag{46}$$

As a numerical example, the model parameter values in Table I were substituted in the equations above. The resulting normalized PDP and FCF are plotted in Figs. 7 and 8, respectively. The average power gain $\bar{G}$ is now six times the expected energy of the first MPC, the mean excess delay $\bar{\tau}$ is 26 ns, and the RMS delay spread σ_τ is 39 ns.

The effect of the averaging over the cluster arrival delays $\{T_l\}$ can be interpreted in a somewhat similar way as the effect

of the averaging over the MPC excess arrival delays $\{\tau_{k,l}\}$ on the PDPs of the individual clusters, as described in the previous subsection. The individual cluster PDPs get dispersed, with increasing dispersion per cluster.

In this particular example we have $\gamma \ll 1/\Lambda$ so that clusters hardly overlap, and $\Gamma \ll 1/\Lambda$ so that the received energy tends to be dominated by the energy received in the first cluster. Therefore, the early part of the overall PDP is dominated by the PDP of the first cluster (which has a known arrival delay $T_0 = 0$, and decays with time constant $\gamma = 20$ ns), while the remaining part consists of the dispersed contributions of the remaining clusters (and decays with time constant $\Gamma = 60$ ns).

Nevertheless, the shape of the overall FCF is also dominated by the first cluster, and is hence nearly equal to the shape of the individual cluster FCF (i.e., the multiplication in the second line of (46) hardly has any influence). The FCF still does not decay to zero for large values of Δf due to the known arrival delay of the first MPC (T_0). The ripple has disappeared because all other arrival delays are now considered unknown.

Basically these results indicate what can be *expected* when nothing is known about the channel realization, except for the arrival delay T_0 of the very first MPC (we will come back to this in Section IV.G) and the type of environment (and hence the model parameter values). Note that a similar argument regarding spatial ergodicity of the cluster arrival delays $\{T_l\}$ can be held as we did in the previous subsection for the MPC excess delays $\{\tau_{k,l}\}$. Hence these analytical results have only little relation with the average results that will be obtained upon spatial averaging around a certain local point, no matter how large the considered area is. At least several different scenarios have to be considered in order to measure a spatial average that will resemble this analytical result.

G. Channel Properties Averaged Over Absolute Arrival Delay

In all analytical expressions derived so far, the actual dependence on the absolute arrival delay T_0 (which is obviously related to the distance between the Tx and Rx) was removed by simply setting it to zero, for convenience. However, as pointed out in footnote 4, we can put the T_0 dependence back in by replacing τ by $\tau - T_0$ in the expressions for the PDP, for instance (42). Likewise, the T_0 dependence of the FCF can be restored by multiplying it by $\exp(-\mathrm{j}\,2\pi\Delta f\, T_0)$.

When the distance between the Tx and Rx is not known, T_0 should be considered as an RV as well. This corresponds to a scenario in which we initially have absolute synchronization between the Tx and RX, and then randomly move one (or both) of them. (This can occur for instance in channel sounding.) The average PDP can be found by averaging the T_0-dependent PDP over T_0. In other words, (42) (or any of the other expressions for PDP, depending on the knowledge of the other RVs) should be convolved with the probability density function of T_0, resulting in a further delay-dispersed PDP, and a narrower FCF that now decays to zero for large values of Δf, because we no longer have any known arrival delays.[15]

[15]Deriving actual expressions requires additional assumptions on the probability density function of T_0, which obviously depends on the joint statistics of the Tx and Rx locations.

H. Average Channel Properties in Case of Large Relative Bandwidths

The situation changes for UWB-REL. First of all, as discussed in Section III.A, the notation with the delta functions in (5) can no longer be applied and should be replaced by (8). The definition in (9) should then be used for the PDP instead of (12), resulting in

$$\begin{aligned} P_h(\tau) &= R_h(\tau,\tau) \\ &= \mathrm{E}\left\{|h(\tau)|^2\right\} \\ &= \sum_{l=0}^{\infty}\sum_{l'=0}^{\infty}\sum_{k=0}^{\infty}\sum_{k'=0}^{\infty} \mathrm{E}\left\{\beta_{k,l}\beta_{k',l'}\exp\left(\mathrm{j}(\phi_{k',l'}-\phi_{k,l})\right)\right. \\ &\quad \left.\cdot\chi^*_{k,l}(\tau - T_l - \tau_{k,l})\,\chi_{k',l'}(\tau - T_{l'} - \tau_{k',l'})\right\}. \end{aligned} \quad (47)$$

The pulse shapes $\{\chi_{k,l}(\cdot)\}$ of the individual MPCs have finite supports and will typically span more than one delay bin in case of UWB-REL. Hence, even when all channel variables $\{\beta_{k,l}, \phi_{k,l}, \tau_{k,l}, T_l\}$ and the pulse shapes $\{\chi_{k,l}(\cdot)\}$ are fully known (i.e., no averaging is performed), we already observe two new phenomena.

1) The autocorrelation terms (the ones with $k = k'$ and $l = l'$, i.e., corresponding to the same MPC) are given by $\beta^2_{k,l}|\chi_{k,l}(\tau - T_l - \tau_{k,l})|^2$ and typically span more than one bin.
2) MPCs will overlap in case the corresponding values of the total arrival delay $T_l + \tau_{k,l}$ differ by an amount that is less than the supports of the individual pulse shapes, resulting in cross-correlations terms, i.e., additional fading in the delay bins where these MPCs overlap.

Second, as discussed in Section III.D, the spatial variation scales of the small-scale fading and the MPC arrival delays are in the same order. In other words, performing the averaging in (47) over the small-scale fading while keeping the MPC arrival delays $\{\tau_{k,l}\}$ fixed (as we did in Section IV.D), has no physical meaning in case of UWB-REL. Without going into further analytical detail, we can see that small spatial variations have several effects on the RVs in (47) and hence several *simultaneous* effects on the PDP.

- The amplitudes $\{\beta_{k,l}\}$ (and phases $\{\phi_{k,l}\}$) fluctuate, due to fluctuations in the small-scale fading (mainly due to phase fluctuations of nonresolvable MPCs).
- The cluster and MPC arrival delays $\{T_l, \tau_{k,l}\}$ also fluctuate, resulting in a fluctuation of the way in which the energy of individual MPCs (the autocorrelation terms) is distributed over different bins, and a fluctuation of the fading in the bins where MPCs overlap (the cross-correlation terms). In short, the fading *statistics* per bin fluctuate.

When spatial averaging is performed, the cross-correlation terms will be attenuated in the observed average PDP, and the fluctuation due to small-scale fading will be more or less averaged out, but the fluctuation of the arrival delays will introduce an additional dispersion of the average autocorrelation terms.

When larger displacements are considered, the MPC interarrival delays can be considered exponentially distributed RVs. Ensemble-averaging will then result in the same PDP and other channel properties as derived in Section IV.E, assuming that the dispersion due to the individual pulse distortions can be neglected compared to the dispersion due to the averaging over the

MPC excess arrival delays. In other words, the result of the ensemble averaging does not depend on the order of the averaging levels.

The additional effects of the pulse distortions and overlapping spatial variation levels have two important consequences for the way in which model parameters are extracted from measurements in case of UWB-REL.

1) It is not possible to fluctuate the Tx and/or Rx position in such a way that independent samples of the fading amplitudes are obtained while fixing the arrival delays and hence the fading *statistics*. Hence it is impossible to derive the fading statistics of resolvable MPCs without tracking individual MPCs and/or resolving MPCs from different directions using an antenna array.
2) It is not possible to average out the effect of small-scale fading from measured PDPs without introducing significant delay dispersion. Next to the unavoidable dispersion due to pulse distortion this will result in a duplication of MPCs when the spatial average is taken, leading to an overestimation of the probability density of small interarrival delays.

V. Conclusion

As proven by measurements in many earlier papers, the SV model is a suitable model for describing the stochastic behavior of the amplitudes, phases and arrival delays of MPCs in WB propagation channels, provided that the scattering objects in the propagation environment are randomly located. In this paper we have given a detailed physical motivation for the structure of the model, showing that the double-Poisson arrivals of MPCs in clusters is a plausible approximation for the channel behavior when the propagation environment contains randomly located "superscatterers" and/or randomly located clusters of scatterers.

The physical motivation has been reconsidered for the case when the SV model is applied to UWB channels. The complex baseband equivalent notation can then still be used, but, for large relative bandwidths, the distortion of the individual MPCs becomes significant, and needs to be modeled explicitly. For large absolute bandwidths, the spatial resolution goes below the size of the dominant scattering objects, introducing correlation between MPCs reflecting upon the same object, and the fading per resolvable MPC can no longer be assumed Rayleigh.

Another important distinction between WB and UWB-REL channels is the overlap of spatial variation scales for small-scale fading and excess arrival delays in UWB-REL channels. In other words, it is not possible to obtain uncorrelated samples of the fading amplitudes (or even average out the effect of fading), while fixing the excess arrival delays and hence the fading statistics. As a result, the statistics of the fading amplitudes and MPC arrival delays cannot be extracted in the same way as for WB channels.

The spatial variation scales and their interpretation were further illustrated by deriving expressions for the channel properties (PDP, mean excess delay, RMS delay spread, and FCF), ensemble-averaged over the fading amplitudes, MPC arrival delays and cluster arrival delays, respectively. These different levels of averaging reflect to what degree the values of the channel variables are known, and correspond to different levels of fluctuation of the Tx, Rx, and scatterer positions.

The notion of these ensemble averaging levels and their relation to the spatial variation levels is important for thoroughly understanding the meaning of the SV model and hence appropriate extraction of the model parameters from measurements, but also for system design and performance evaluation.

Acknowledgment

The authors would like to thank the reviewers for their valuable comments that have greatly contributed to improving the quality of the manuscript.

Opinions expressed in this paper are those of the authors and do not reflect those of the Office of Naval Research or the National Science Foundation.

References

[1] A. A. M. Saleh and R. A. Valenzuela, "A statistical model for indoor multipath propagation," *IEEE J. Sel. Areas Commun.*, vol. SAC-5, pp. 128–137, Feb. 1987.
[2] A. F. Molisch, J. R. Foerster, and M. Pendergrass, "Channel models for ultrawideband personal area networks," *IEEE Wireless Commun.*, vol. 10, no. 6, pp. 14–21, Dec. 2003.
[3] J. R. Foerster, "Channel modeling Subcommittee report final," Tech. Rep. P802.15 02/490r1, IEEE 802.15 SG3a, Feb. 2003.
[4] A. F. Molisch *et al.*, "A comprehensive model for ultrawideband propagation channels," *IEEE Trans. Antennas Propag.*, vol. 54, no. 11, pp. 3151–3166, Nov. 2006.
[5] A. F. Molisch *et al.*, "IEEE 802.15.4a channel model—Final report," Tech. Rep. Doc. IEEE 802.15-04-0662-02-004a, 2005.
[6] A. F. Molisch, "Ultra-wide-band propagation channels," *Proc. IEEE*, vol. 97, no. 2, pp. 353–371, Feb. 2009.
[7] N. Michelusi, U. Mitra, A. F. Molisch, and M. Zorzi, "UWB sparse/diffuse channels—Part I: Channel models and Bayesian estimators," *IEEE Trans. Signal Process.*, vol. 60, no. 10, pp. 5307–5319, Oct. 2012.
[8] G. L. Turin, "Communication through noisy, random-multipath channels," in *IRE Conven. Rec.*, 1956, pp. 154–166, pt. 4.
[9] G. L. Turin *et al.*, "A statistical model for urban multipath propagation," *IEEE Trans. Veh. Technol.*, vol. VT-21, no. 1, pp. 1–9, Feb. 1972.
[10] H. Suzuki, "A statistical model for urban radio propagation," *IEEE Trans. Commun.*, vol. COM-25, no. 7, pp. 673–680, Jul. 1977.
[11] H. Hashemi, "The indoor radio propagation channel," *Proc. IEEE*, vol. 81, no. 7, pp. 943–968, Jul. 1993.
[12] J. Neyman and E. L. Scott, "Statistical approach to problems of cosmology," *J. Royal Stat. Soc.*, vol. 20, no. 1, pp. 1–43, 1958.
[13] J. Neyman and E. L. Scott, "A theory of the spatial distribution of galaxies," *Astrophys. J.*, vol. 116, pp. 144–163, 1952.
[14] A. F. Molisch, *Wireless Communications*. New York, NY, USA: Wiley, 2005.
[15] P. A. Bello, "Characterization of randomly time-variant linear channels," *IEEE Trans. Commun.*, vol. COM-11, no. 4, pp. 360–393, Dec. 1963.
[16] K. Haneda, A. Richter, and A. F. Molisch, "Modeling the frequency dependence of ultra-wideband spatio-temporal indoor radio channels," *IEEE Trans. Antennas Propag.*, vol. 60, no. 6, pp. 2940–2950, Jun. 2012.
[17] C.-C. Chong, Y. Kim, and S. S. Lee, "A modified S-V clustering channel model for the UWB indoor residential environment," *Proc. IEEE VTC Spring*, pp. 58–62, 2005.
[18] C.-C. Chong and S. K. Yong, "A generic statistical-based UWB channel model for high-rise apartments," *IEEE Trans. Antennas Propag.*, vol. 53, no. 8, pp. 2389–2399, Aug. 2005.
[19] D. Cassioli, M. Z. Win, and A. F. Molisch, "The ultra-wide bandwidth indoor channel: From statistical model to simulations," *IEEE J. Sel. Areas Commun.*, vol. 20, no. 6, pp. 1247–1257, Aug. 2002.
[20] W. Q. Malik, B. Allen, and D. J. Edwards, "Bandwidth-dependent modelling of small-scale fade depth in wireless channels," *IET Microw. Antennas Propag.*, vol. 2, no. 6, pp. 519–528, Sep. 2008.
[21] M. L. Jakobsen, T. Pedersen, and B. H. Fleuri, "Analysis of the stochastic channel model by Saleh & Valenzuela via the theory of point processes," presented at the Int. Zurich Seminar Commun. (IZS), Zurich, Switzerland, Feb. 29–Mar. 2 2012.
[22] G. Llano, J. Reig, and L. Rubio, "The UWB-OFDM channel analysis in frequency," presented at the IEEE 69th Veh. Technol. Conf. (VTC Spring), Barcelona, Spain, Apr. 26–29, 2009.

[23] M. Derpich and R. Feick, "On the second-order power spectral statistics of wideband indoor microwave channels," presented at the IEEE 21st Int. Symp. Pers. Indoor Mobile Radio Commun. (PIMRC 2010), Istanbul, Turkey, Sep. 26–29, 2010.

Arjan Meijerink (S'00–M'06–SM'11) was born in Almelo, The Netherlands, in 1976. He received the M.Sc. and Ph.D. degrees in electrical engineering (both with honors) from the University of Twente, Enschede, The Netherlands, in 2001 and 2005, respectively.

In 2000, he was a Trainee at Ericsson Business Mobile Networks, Enschede, The Netherlands, developing error concealment techniques for Bluetooth voicelinks. From 2001 to 2005, he was a Research Assistant in the Telecommunication Engineering Group at the University of Twente, carrying out his Ph.D. research on optical coherence multiplexing. From 2005 to 2007, he was a Postdoctoral Researcher in the same group, working on RF photonic signal processing techniques, especially on the design and performance analysis of fully integrated ring resonator-based optical beamformers. Since 2007, he has been an Assistant Professor in the Telecommunication Engineering Group, where he is involved in research on new short-range radio transmission techniques for wireless ad-hoc networks. In 2009, he was a Visiting Lecturer in the Wireless Communications Research Group at the Queen's University in Belfast, U.K., and in 2010 he was a Visiting Scholar in the Wireless Devices and Systems Group at the University of Southern California in Los Angeles, CA, USA.

Dr. Meijerink is a Member of the IEEE Communications Society and the International Union of Radio Science URSI, and has served as a Reviewer for various journals, conferences, and symposia. Currently, he is Junior Past Secretary of the IEEE Benelux Section, and he is a Member of the Executive Committee of the IEEE Benelux Joint Chapter on Communication and Vehicular Technology.

Andreas F. Molisch (S'89–M'95–SM'00–F'05) received the Dipl. Ing., Dr. Techn., and habilitation degrees from the Technical University (TU) Vienna, Austria, in 1990, 1994, and 1999, respectively.

From 1991 to 2000, he was with the TU Vienna, becoming an Associate Professor there in 1999. From 2000 to 2002, he was with the Wireless Systems Research Department at AT&T (Bell) Laboratories Research in Middletown, NJ, USA. From 2002 to 2008, he was with Mitsubishi Electric Research Labs, Cambridge, MA, USA, most recently as Distinguished Member of Technical Staff and Chief Wireless Standards Architect. Concurrently he was also Professor and Chairholder for Radio Systems at Lund University, Lund, Sweden. Since 2009, he has been Professor of Electrical Engineering at the University of Southern California, Los Angeles, CA, USA, where he heads the Wireless Devices and Systems (WiDeS) group. Since 2011, he has also been codirector of the Communications Sciences Institute (CSI). He has authored, coauthored or edited four books—among them the textbook "Wireless Communications," (Wiley–IEEE Press, 2nd ed., 2011)—16 book chapters, about 170 journal papers, and numerous conference contributions, as well as more than 70 patents and 60 standards contributions. He has done research in the areas of SAW filters, radiative transfer in atomic vapors, atomic line filters, smart antennas, and wideband systems. His current research interests are measurement and modeling of mobile radio channels, UWB, cooperative communications, MIMO systems, and wireless healthcare.

Dr. Molisch is a Fellow of the IET, Fellow of the AAAS, and an IEEE Distinguished Lecturer, as well as a member of the Austrian Academy of Sciences. He was Area Editor for Antennas and Propagation of the IEEE TRANSACTIONS ON WIRELESS COMMUNICATIONS, Division Editor of the IEEE/KICS JOURNAL OF COMMUNICATIONS AND NETWORKS, and coeditor of special issues of several journals. He has been General Chair, TPC Chair, or Track/Symposium Chair of numerous international conferences. He was chairman of the COST 273 working group on MIMO channels, the IEEE 802.15.4a channel model standardization group, Commission C (signals and systems) of URSI (International Union of Radio Scientists, 2005–2008), and the Radio Communications Committee of the IEEE Communications Society (2009–2010). He has received numerous awards, most recently the Donald Fink Award of the IEEE and the Eric Sumner Award of the IEEE.